Latin American Journal of Solids and Structures
www.lajss.org

Application of an improved three-phase model to calculate effective characteristics for a composite with cylindrical inclusions

Abstract

A modified three-phase composite model yielding reliable effective characteristics of composite structures has been proposed. In particular, the problem of effective heat transfer coefficient of the composite structure with periodically located inclusions of circular cross-sections located on a square net is solved. Advantages of the proposed model in comparison to the classical three-phase model are illustrated and discussed.

Keywords

Composite, three-phase model, periodic inclusions, heat transfer

Igor V. Andrianov[1], **Jan Awrejcewicz**[2], **Galina A. Starushenko**[3]

[1] Institute of General Mechanics, RWTH Aachen University, Templergraben 64, D-52056, Aachen, Germany
[2] Technical University of Łódź, Department of Automation and Biomechanics, 1/15 Stefanowski St., PL-90-924, Łódź, Poland
[3] Dnipropetrovs'k Regional Institute of State Management of National Academy of State Management at the President of Ukraine, Gogolya 29, UA-49631, Dnipropetrovs'k, Ukraine

1 INTRODUCTION

The three-phase model of a composite (TPhM) has been used in references [2-5,10,11,15-17] in order to define effective characteristics of composite structures. The physical meaning of the idealization introduced by TPhM relies on substitution of the periodic structure being studied by its counterpart homogeneous homogenized structure with the equivalently reduced parameters (to be defined) except of only one characteristic structure cell. Further step of the solution requires derivation of mathematical formulas regarding homogenized coefficients through the application of physical understanding and mainly via either the energy principle [4,5,10,11,17] or structure geometry [2,3,15,16].

In particular, in the problem devoted to determination of the equivalent heat transfer coefficient of a two-phase composite structure with periodic cylindrical inclusions of circular cross-sections located on a square net the analysis revealed the following essential features:

(i) For small inclusions size $a << 1$ heat transfer parameter λ is validated for its arbitrary values;
(ii) For large inclusion size $a \to 1$ the TPhM model yields reliable results assuming that heat transfer of the inclusions is of the order of structure matrix $\lambda \sim 1$;

(iii) TPhM may yield even a qualitatively wrong result for either large inclusion size $a \to 1$ or large/small conductivity properties, i.e. for $\lambda \to \infty$ and $\lambda \to 0$.

A construction of the first order TPhM approximation using the method of variations of boundary shapes of the studied structure does not allow us to overcome the earlier mentioned problems, in particular with respect to the possible wide spectrum of applications. Furthermore, a solution being limited to the first inclusion approximation does not describe the structure properties adequately for large values of the inclusion size. Namely, it does not allow achieving even a qualitative picture of the processes which occur in the composite (for example, a validation of the infinite cluster occurrence). The latter commentary can also be expressed mathematically. Namely, the first terms of the asymptotic series do not influence the further asymptotic sequence being defined through a zero order approximation.

In this work novel algorithms associated with the application of the composite TPhM are developed. The main idea and advantages of our proposal are illustrated and discussed taking as an example a solution to the heat transfer problem of the composite structure with cylindrical inclusions of circular cross-sections.

2 SOLVING THE HEAT TRANSFER PROBLEM WITH THE USE OF THE IMPROVED COMPOSITE TPHM

The problem of determination of effective coefficients of the micro non-homogeneous material consisting of a continuous matrix and periodically located cylindrical inclusions with circular cross-sections is solved in this work. In our study structure size in the direction of the fibre length essentially exceed the remaining size, i.e. $L >> \ell$ (Figure 2.1).

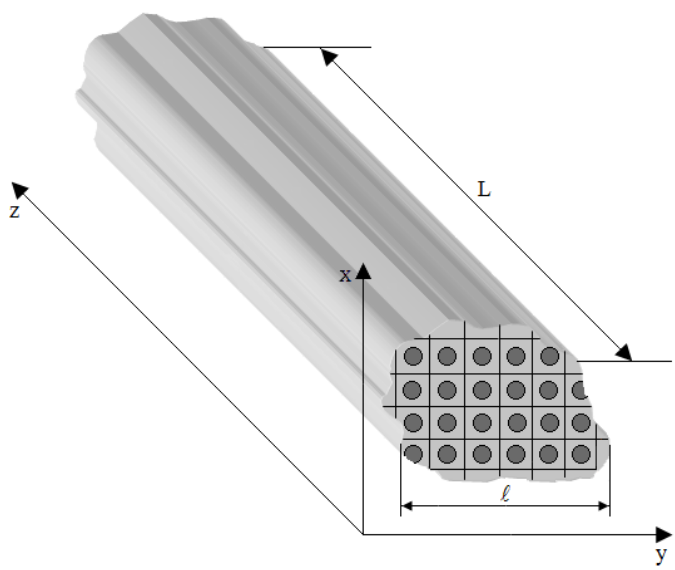

Fig. 2.1. Composite structure with periodically located cylindrical inclusions of circular cross-sections.

We assume that the studied structure is two-periodic with the same period in both directions and the inclusions are located within the square net. Period $2b$ is small in comparison with the characteristic diameter of the composite cross-section, i.e. $2b << \ell$.

Phases of the composite have different heat transfer coefficients λ^+ and λ^- in the matrix (area Ω_i^+) and inclusions (area Ω_i^-), respectively, where $\dfrac{\lambda^-}{\lambda^+} = \lambda$. The characteristic of the periodically repeated cell composite is shown in Figure 2.2.

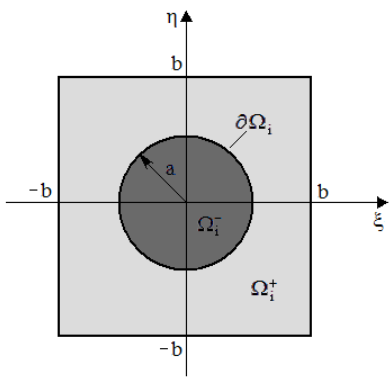

Fig. 2.2. A periodically repeated cell of the composite.

Material behaviour in the area of Ω_i^+ and Ω_i^- is governed by the Poisson equations of the following form

$$\lambda^+ \Delta u^+ = F \quad \text{in} \quad \Omega_i^+; \tag{2.1}$$

$$\lambda^- \Delta u^- = F \quad \text{in} \quad \Omega_i^-, \tag{2.2}$$

where u^+, u^- are the functions of temperature distributions regarding the mentioned areas; F stands for the density of heat sources.

In the interface of the matrix with inclusions the following compatibility conditions hold:

$$u^+ = u^- \quad \text{on} \quad \partial\Omega_i; \tag{2.3}$$

$$\lambda^+ \quad \frac{\partial u^+}{\partial \mathbf{n}} = \lambda^- \quad \frac{\partial u^-}{\partial \mathbf{n}} \quad \text{on} \quad \partial\Omega_i, \tag{2.4}$$

where $\mathbf{n}$ denotes a contour normal to the inclusion.

Solution to the boundary value problems (2.1)-(2.4), owing to the homogenization method [12], can be presented in the form of the asymptotic series with respect to a small parameter ε of the following form:

$$u^{\pm} = u_0(x,y) + \varepsilon\, u_1^{\pm}(x,y,\xi,\eta) + \varepsilon^2 u_2^{\pm}(x,y,\xi,\eta) + \dots ,$$

where x, y are slow variables, having a measurement in the interval of the whole composite structure space; ξ, η are fast variables, describing the problem on the structure cell and $\varepsilon << 1$ is the small parameter characterizing the composite periodicity.

1. Solution to the problem is constructed using the modernized three-phase composite model (TPhMM) being characterised by the following properties: the whole composite structure , except one cell, is substituted by the equivalent homogeneous medium $\tilde{\Omega}$ having the known (to be found) heat transfer coefficient $\tilde{\lambda}$. Furthermore, we introduce two circles to describe the square matrix cell contour with the following radii (see Figure 2.3):

$$r = \begin{cases} b\ \eta\ = \sqrt{1+\eta^2}\,, \ 0 \le \eta \le 1 \quad \text{for} \quad 0 \le \theta \le \dfrac{\pi}{4} \\ b\ \xi\ = \sqrt{1+\xi^2}\,, \ 0 \le \xi \le 1 \quad \text{for} \quad \dfrac{\pi}{4} \le \theta \le \dfrac{\pi}{2} \end{cases} \tag{2.5}$$

The cell problem in polar coordinates $r,\ \theta$ can be cast to the following form [16]:

$$\frac{\partial^2 u_1^+}{\partial r^2} + \frac{1}{r}\cdot\frac{\partial u_1^+}{\partial r} + \frac{1}{r^2}\cdot\frac{\partial^2 u_1^+}{\partial \theta^2} = 0 \ \ in \ \ \Omega_i^+ \tag{2.6}$$

$$\frac{\partial^2 u_1^-}{\partial r^2} + \frac{1}{r}\cdot\frac{\partial u_1^-}{\partial r} + \frac{1}{r^2}\cdot\frac{\partial^2 u_1^-}{\partial \theta^2} = 0 \ \ in \ \ \Omega_i^- \tag{2.7}$$

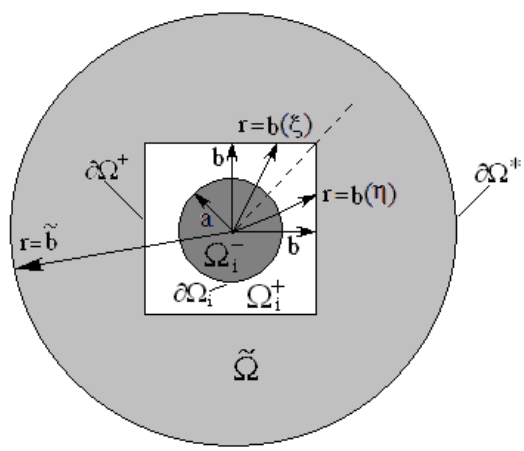

Fig. 2.3. Mapping of a square cell contour into TPhMM.

$$\frac{\partial^2 \tilde{u}_1}{\partial r^2} + \frac{1}{r} \cdot \frac{\partial \tilde{u}_1}{\partial r} + \frac{1}{r^2} \cdot \frac{\partial^2 \tilde{u}_1}{\partial \theta^2} = 0 \quad in \quad \tilde{\Omega} \tag{2.8}$$

$$u_1^+ = u_1^-; \ \frac{\partial u_1^+}{\partial r} - \lambda \frac{\partial u_1^-}{\partial r} = \ \lambda - 1 \left(\frac{\partial u_0}{\partial x} \cos\theta + \frac{\partial u_0}{\partial y} \sin\theta \right) \ for \ \ r = a \tag{2.9}$$

$$u_1^+ = \tilde{u}_1; \ \frac{\partial u_1^+}{\partial r} - \tilde{\lambda} \frac{\partial \tilde{u}_1}{\partial r} = \ \tilde{\lambda} - 1 \left(\frac{\partial u_0}{\partial x} \cos\theta + \frac{\partial u_0}{\partial y} \sin\theta \right) \ for \ \ r = b \tag{2.10}$$

$$\tilde{u}_1 \to 0; \ \frac{\partial \tilde{u}_1}{\partial r} \to 0 \ \ for \ \ r = \tilde{b} \to \infty \tag{2.11}$$

The solution to the boundary value problem (2.6)-(2.11) is as follows:

$$\begin{aligned} u_1^- &= A_1 r \cos\theta + A_2 r \sin\theta, \\ u_1^+ &= \left(B_1 r + \frac{C_1}{r} \right) \cos\theta + \left(B_2 r + \frac{C_2}{r} \right) \sin\theta, \\ \tilde{u}_1 &= \frac{D_1}{r} \cos\theta + \frac{D_2}{r} \sin\theta, \end{aligned} \tag{2.12}$$

where

$$\begin{aligned} A_1 &= -\left(1 + \frac{4\tilde{\lambda} b^2}{\tilde{\lambda} - 1 \quad \lambda - 1 \ a^2 - \ \tilde{\lambda} + 1 \quad \lambda + 1 \ b^2} \right) \frac{\partial u_0}{\partial x}, \\ B_1 &= -\left(1 + \frac{2\tilde{\lambda} \ \lambda + 1 \ b^2}{\tilde{\lambda} - 1 \quad \lambda - 1 \ a^2 - \ \tilde{\lambda} + 1 \quad \lambda + 1 \ b^2} \right) \frac{\partial u_0}{\partial x}, \\ C_1 &= \frac{2\tilde{\lambda} \ \lambda - 1 \ a^2 b^2}{\tilde{\lambda} - 1 \quad \lambda - 1 \ a^2 - \ \tilde{\lambda} + 1 \quad \lambda + 1 \ b^2} \frac{\partial u_0}{\partial x}, \\ D_1 &= b^2 \left(1 + 2 \frac{\lambda + 1 \ b^2 + \ \lambda - 1 \ a^2}{\tilde{\lambda} - 1 \quad \lambda - 1 \ a^2 - \ \tilde{\lambda} + 1 \quad \lambda + 1 \ b^2} \right) \frac{\partial u_0}{\partial x}, \\ A_2 &= A_1, \ B_2 = B_1, \ C_2 = C_1, \ D_2 = D_1 \ \left(\frac{\partial u_0}{\partial x} \to \frac{\partial u_0}{\partial y} \right). \end{aligned} \tag{2.13}$$

Observe that during the homogenization procedure subjected to the equation

$$\frac{\partial^2 u_0}{\partial x^2}+\frac{\partial^2 u_0}{\partial y^2}+2\frac{\partial^2 u_1^+}{\partial x\partial\xi}+2\frac{\partial^2 u_1^+}{\partial y\partial\eta}+\frac{\partial^2 u_2^+}{\partial\xi^2}+\frac{\partial^2 u_2^+}{\partial\eta^2}+\lambda\left(\frac{\partial^2 u_0}{\partial x^2}+\frac{\partial^2 u_0}{\partial y^2}+2\frac{\partial^2 u_1^-}{\partial x\partial\xi}+\right.$$
$$\left.2\frac{\partial^2 u_1^-}{\partial y\partial\eta}+\frac{\partial^2 u_2^-}{\partial\xi^2}+\frac{\partial^2 u_2^-}{\partial\eta^2}\right)+\tilde{\lambda}\left(\frac{\partial^2 u_0}{\partial x^2}+\frac{\partial^2 u_0}{\partial y^2}+2\frac{\partial^2 \tilde{u}_1}{\partial x\partial\xi}+2\frac{\partial^2 \tilde{u}_1}{\partial y\partial\eta}+\frac{\partial^2 \tilde{u}_2}{\partial\xi^2}+\frac{\partial^2 \tilde{u}_2}{\partial\eta^2}\right)=F,$$

the integration is carried out using Eq. (2.5), i.e. in formula (2.13) we take

$$b=\begin{cases} b\ \ \xi\ \ =\sqrt{1+\xi^2},\ \ 0\le\xi\le 1 \quad \text{in} \quad \Omega_{i1}^+,\Omega_{i1}^-,\tilde{\Omega}_1 \\ b\ \ \eta\ \ =\sqrt{1+\eta^2},\ \ 0\le\eta\le 1 \quad \text{in} \quad \Omega_{i2}^+,\Omega_{i2}^-,\tilde{\Omega}_2 \end{cases} \tag{2.14}$$

In Figure 2.4 a quadrant of the three phase area is shown, where the integration via the TPhMM is carried out.

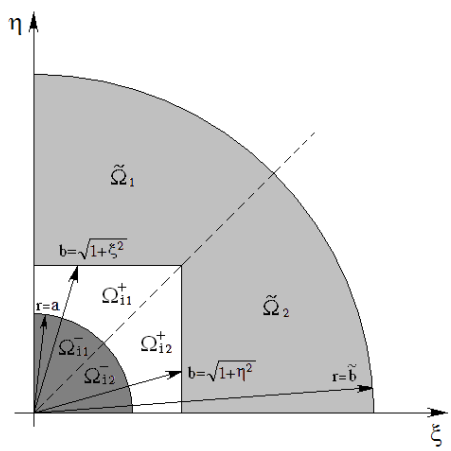

Fig. 2.4. Approximation of the three phase area used in TPhMM.

After integration using Eqs. (2.13), (2.14) and the following formula

$$\frac{1}{\left|\Omega^{*}\right|}\left[\iint\limits_{\Omega_i^+}\left(\frac{\partial^2 u_0}{\partial x^2}+\frac{\partial^2 u_0}{\partial y^2}+\frac{\partial^2 u_1^+}{\partial x\partial\xi}+\frac{\partial^2 u_1^+}{\partial y\partial\eta}\right)d\xi\,d\eta+\lambda\iint\limits_{\Omega_i^-}\left(\frac{\partial^2 u_0}{\partial x^2}+\frac{\partial^2 u_0}{\partial y^2}+\frac{\partial^2 u_1^-}{\partial x\partial\xi}+\frac{\partial^2 u_1^-}{\partial y\partial\eta}\right)d\xi\,d\eta+\right.$$
$$\left.\tilde{\lambda}\iint\limits_{\tilde{\Omega}}\left(\frac{\partial^2 u_0}{\partial x^2}+\frac{\partial^2 u_0}{\partial y^2}+\frac{\partial^2 \tilde{u}_1}{\partial x\partial\xi}+\frac{\partial^2 \tilde{u}_1}{\partial y\partial\eta}\right)\ d\xi\quad d\eta\right]=F\,,$$

where

$$\Omega_i^{\pm} = \Omega_{i1}^{\pm} \cup \Omega_{i2}^{\pm}\,,\ \tilde{\Omega} = \tilde{\Omega}_1 \cup \tilde{\Omega}_2\,,\ \left|\,\Omega^*\,\right| = \left|\,\Omega_i^+ \cup \Omega_i^- \cup \tilde{\Omega}\,\right|,$$

and after satisfying the necessary conditions, the following transcendental equation is derived defining heat transfer coefficient $\tilde{\lambda}$:

$$\tilde{\lambda} = \frac{1 + \left(\frac{1}{\Delta} - \Delta\right)\arctan\frac{1}{\Delta} + \frac{\lambda - 1}{\lambda + 1}\frac{a^2}{\Delta}\arctan\frac{1}{\Delta}}{1 + \left(\frac{1}{\Delta} - \Delta\right)\arctan\frac{1}{\Delta} - \frac{\lambda - 1}{\lambda + 1}\frac{a^2}{\Delta}\arctan\frac{1}{\Delta}} \tag{2.15}$$

where

$$\Delta = \sqrt{1 - \frac{\tilde{\lambda} - 1}{\tilde{\lambda} + 1} \cdot \frac{\lambda - 1}{\lambda + 1} a^2} \tag{2.16}$$

Transcendental Eqs. (2.15), (2.16) can be solved numerically in spite of the limiting values of the heat conductivity parameter: $\lambda \to \infty, a \to 1$ and $\lambda \to 0, a \to 1$. In the latter case it is worthwhile to use the asymptotic representations, which can be obtained on the basis of relations (2.15) and (2.16).

3 ASYMPTOTIC RELATIONS FOR THE EQUIVALENT HEAT TRANSFER PARAMETER

1) The equivalent heat transfer parameter obtained from the transcendental equations (2.15)-(2.16) satisfies Keller's theorem [9]:

$$\tilde{\lambda}\ \lambda\ = \tilde{\lambda}^{-1}\ \lambda^{-1} \tag{3.1}$$

Indeed, we have

$$\tilde{\lambda}^{-1}\ \lambda^{-1}\ = \left(\frac{1 + \left(\frac{1}{\Delta} - \Delta\right)\arctan\frac{1}{\Delta} + \frac{\lambda - 1}{\lambda + 1}\frac{a^2}{\Delta}\arctan\frac{1}{\Delta}}{1 + \left(\frac{1}{\Delta} - \Delta\right)\arctan\frac{1}{\Delta} - \frac{\lambda - 1}{\lambda + 1}\frac{a^2}{\Delta}\arctan\frac{1}{\Delta}}\right)^{-1} =$$
$$= \frac{1 + \left(\frac{1}{\Delta} - \Delta\right)\arctan\frac{1}{\Delta} - \frac{\lambda - 1}{\lambda + 1}\frac{a^2}{\Delta}\arctan\frac{1}{\Delta}}{1 + \left(\frac{1}{\Delta} - \Delta\right)\arctan\frac{1}{\Delta} + \frac{\lambda - 1}{\lambda + 1}\frac{a^2}{\Delta}\arctan\frac{1}{\Delta}}$$

where

$$\Delta\ \tilde{\lambda}^{-1}, \lambda^{-1}\ = \Delta\ \tilde{\lambda}, \lambda\ ,$$

and hence (3.1) has been proved.

Furthermore, the structure of equations (2.15) and (2.16) allows for a direct use of Δ as a natural small parameter $0 \le \Delta \le 1$ for arbitrary values of $0 \le \lambda < \infty$ and $0 \le a \le 1$.

Now, having this parameter one may define and investigate further the limiting transitions.

2) Let us investigate a composite having heat transfer of the matrix and inclusions of the same order, i.e.

$\lambda \to 1$.

In this case for arbitrary values of the inclusion size we have:

$$\tilde{\lambda} \sim 1 \quad \Rightarrow \quad \Delta \to 1.$$

It implies that transcendental Eqs. (2.15) and (2.16) can be reduced to the following forms:

2.1) For inclusions of small geometric size $a \to 0$:

$$\tilde{\lambda} = 1 + \ \lambda - 1\ \frac{\pi a^2}{4}.$$

2.2) For inclusions of large geometric size $a \to 1$:

$$\tilde{\lambda} = 1 + \frac{\pi\ \lambda - 1}{4} - \frac{\pi\ \lambda - 1}{2}\ 1 - a\ .$$

3) Let us study the case of the absolute heat transfer, i.e. when $\lambda \to \infty$.

3.1) If size of the inclusions are small, i.e. when $a \to 0$, we have

$$\tilde{\lambda} \sim 1 \quad \Rightarrow \quad \Delta \to 1,$$

and consequently

$$\tilde{\lambda} = 1 + \left(1 - \frac{2}{\lambda}\right)\frac{\pi\, a^2}{2}.$$

3.2) We study the case of inclusions of large geometric size $0 << a < 1$.

The physical meaning of the problem implies that in the case of inclusions with infinitely high heat transfer properties $\lambda \to \infty$ and geometric size close to the limiting large ones of the order $a \sim 1$, the homogenized heat transfer coefficient $\tilde{\lambda}$ is also infinitely large, i.e.

$$\tilde{\lambda} \to \infty \quad \Rightarrow \quad \Delta \to 0 .$$

Therefore, transcendental Eqs. (2.15) and (2.16) are transformed to the following form

$$\tilde{\lambda} = 1 + \frac{2a^2}{\sqrt{1-a^2}} \arctan \frac{1}{\sqrt{1-a^2}} \tag{3.2}$$

and for $a \to 1$ one obtains

$$\tilde{\lambda} = \frac{\pi}{\sqrt{1-a^2}} - 1 \tag{3.3}$$

It should be emphasized that the main term of the series development (3.3) coincides with the asymptotic representation q^{∞}_{asympt}, reported in [13] (with accuracy of the normalisation introduced in [13]) for the effective heat transfer of a composite with circular cross-sections of large cylindrical inclusions having absolute heat transfer properties.

4) Below, we study the entirely resistant heat transfer inclusions, i.e. these with $\lambda \to 0$.

4.1) For small additives $a \to 0$ we have $\tilde{\lambda} \sim 1 \quad \Rightarrow \quad \Delta \to 1$, and consequently

$$\tilde{\lambda} = 1 - \ 1 - 2\lambda \ \frac{\pi a^2}{2} \tag{3.4}$$

Formula (3.4) for $\lambda = 0$ coincides (with accuracy up to the terms of the order of a^2) with the results obtained in [1] for the effective heat transfer of the composite consisting of inclusions without heat transfer property.

4.2) Large inclusions $0 << a < 1$.

Proceeding in the way analogous to that presented in Section 3.2, we may trace the limiting transition exhibited by relations of the equivalent heat transfer parameter defined by Eqs. (2.15), (2.16) for the non-conductive heat inclusions of large sizes: $\lambda \to 0$; $a \sim 1$. In this case the homogenized heat transfer coefficient $\tilde{\lambda}$ will be infinitely small, i.e. $\tilde{\lambda} \to 0 \quad \Rightarrow \quad \Delta \to 0$.

As a result we obtain

$$\tilde{\lambda} = \frac{1}{1 + \dfrac{2a^2}{\sqrt{1-a^2}} \arctan \dfrac{1}{\sqrt{1-a^2}}} \tag{3.5}$$

and for $a \to 1$ we get

$$\tilde{\lambda} = \frac{\sqrt{1-a^2}}{\pi - \sqrt{1-a^2}} \tag{3.6}$$

5) Next, we consider a composite with small size inclusions, i.e. $a \to 0$.

Motivated by physical properties one may conclude that for the case of arbitrary heat transfer values $0 < \lambda < \infty$, including the infinite large $\lambda \to \infty$ and infinitely small $\lambda = 0$ values, the homogenized heat transfer is:

$$\tilde{\lambda} \sim 1 \quad \Rightarrow \quad \Delta \to 1 .$$

Therefore we finally obtain:

5.1) For inclusions of infinitely large heat transfer property $\lambda \to \infty$ we have

$$\tilde{\lambda} = 1 + \frac{\pi a^2}{2} - \frac{\pi a^2}{\lambda} .$$

5.2) For inclusions of infinitely small $\lambda \to 0$ we have

$$\tilde{\lambda} = 1 - \frac{\pi a^2}{2} + \pi a^2 \lambda .$$

5.3) For inclusions with $\lambda \sim 1$ we have

$$\tilde{\lambda} = 1 + \frac{\pi a^2}{4} \ \lambda - 1 \ .$$

6) In the case of the composite structure with inclusions of large size $a \to 1$ and for $0 \le \lambda < \infty$ the equivalent homogenized heat transfer $\tilde{\lambda}$ satisfies the following relation

$$\frac{\tilde{\lambda} - 1}{\tilde{\lambda} + 1} \sim \frac{\lambda - 1}{\lambda + 1},$$

which means that

$$\frac{\tilde{\lambda}-1}{\tilde{\lambda}+1} \sim \frac{\lambda-1}{\lambda+1} \sim -1 \text{ for } \lambda \to 0\,,$$
$$\frac{\tilde{\lambda}-1}{\tilde{\lambda}+1} \sim \frac{\lambda-1}{\lambda+1} \sim 0 \text{ for } \lambda \sim 1\,,$$
$$\frac{\tilde{\lambda}-1}{\tilde{\lambda}+1} \sim \frac{\lambda-1}{\lambda+1} \sim 1 \text{ for } \lambda \to \infty\,.$$

Then the transcendental Eq. (2.15) yields a relation to determine $\tilde{\lambda}$ where the formula for Δ in Eq. (2.16) takes the form

$$\Delta = \sqrt{1-\left(\frac{\lambda-1}{\lambda+1}\right)^2 a^2} \tag{3.7}$$

In particular we have:

6.1) for inclusions of large heat transfer $\lambda >> 1$:

$$\tilde{\lambda} = \frac{\pi}{\sqrt{2}}\sqrt{\lambda} - 1\,,$$

6.2) for inclusions of small heat transfer $\lambda << 1$:

$$\tilde{\lambda} = \frac{\sqrt{2}}{\pi}\sqrt{\lambda} + \frac{2}{\pi^2}\lambda\,,$$

6.3) for inclusions of heat transfer of the order of the matrix heat transfer $\lambda \sim 1$:

$$\tilde{\lambda} = 1 + \frac{\pi}{4}\ \lambda - 1\ .$$

4 RESULTS OF COMPUTATION OF THE EFFECTIVE HEAT TRANSFER COEFFICIENT FOUND USING TPHMM

1) In Figures 3.1 to 3.10 graphs of the homogenized heat transfer coefficient yielded by the TPhMM for various values of the heat transfer inclusions λ are reported:

$\lambda << 1 \quad \lambda = 10^{-2};\ \lambda = 10^{-1}$, see Figures 4.1 and 4.2.

$\lambda < 1 \quad \lambda = 0.2;\ \lambda = 0.5$, see Figures 4.3 and 4.4.

$\lambda \sim 1 \quad \lambda = 0.8;\ \lambda = 1.25$, see Figures 4.5 and 4.6.

$\lambda > 1 \quad \lambda = 2;\ \lambda = 5$, see Figures 4.7 and 4.8.

$\lambda >> 1 \quad \lambda = 10;\ \lambda = 10^2$, see Figures 4.9 and 4.10.

In order to compare the obtained results, the Hashin-Shtrickman (H-S) boundaries are also reported [6, 7, 18] which are defined through the following relations

$$\frac{1-\frac{\pi a^2}{4b^2}+\lambda\left(1+\frac{\pi a^2}{4b^2}\right)}{1+\frac{\pi a^2}{4b^2}+\lambda\left(1-\frac{\pi a^2}{4b^2}\right)} = \underline{q}_{H-S} \le q \le \bar{q}_{H-S} = \lambda\frac{2-\frac{\pi a^2}{4b^2}+\lambda\frac{\pi a^2}{4b^2}}{\frac{\pi a^2}{4b^2}+\lambda\left(2-\frac{\pi a^2}{4b^2}\right)} \quad \text{for } 1 \le \lambda < \infty; \tag{4.1}$$

$$\lambda\frac{2-\frac{\pi a^2}{4b^2}+\lambda\frac{\pi a^2}{4b^2}}{\frac{\pi a^2}{4b^2}+\lambda\left(2-\frac{\pi a^2}{4b^2}\right)} = \underline{q}_{H-S} \le q \le \bar{q}_{H-S} = \frac{1-\frac{\pi a^2}{4b^2}+\lambda\left(1+\frac{\pi a^2}{4b^2}\right)}{1+\frac{\pi a^2}{4b^2}+\lambda\left(1-\frac{\pi a^2}{4b^2}\right)} \quad \text{for } 0 \le \lambda \le 1. \tag{4.2}$$

It is worth noting that the solution obtained via the TPhM identically coincides with the lower boundary of the H-S estimation for $1 \le \lambda < \infty$ and regarding the upper boundary for $0 \le \lambda \le 1$.

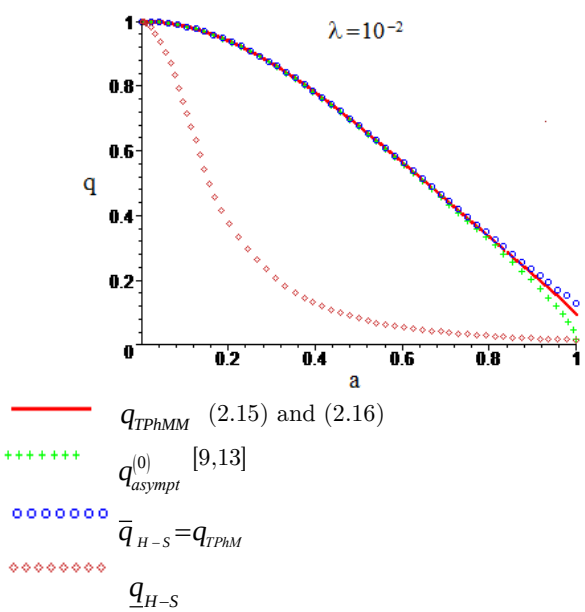

Fig. 4.1. Homogenized heat transfer coefficient for $\lambda = 10^{-2}$.

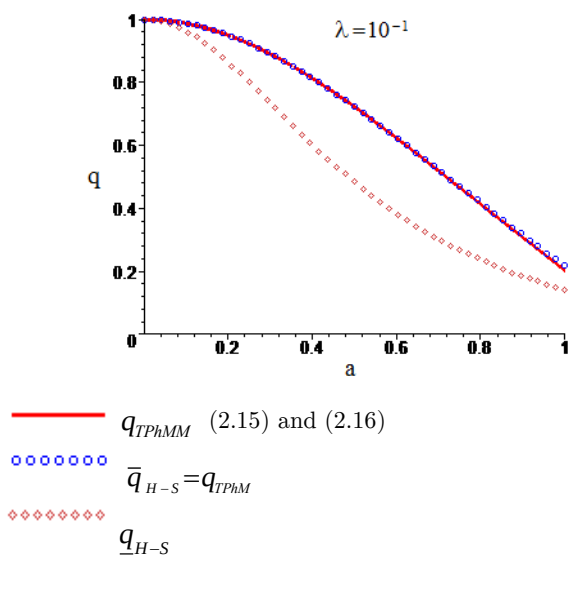

Fig. 4.2. Homogenized heat transfer coefficient for $\lambda = 10^{-1}$.

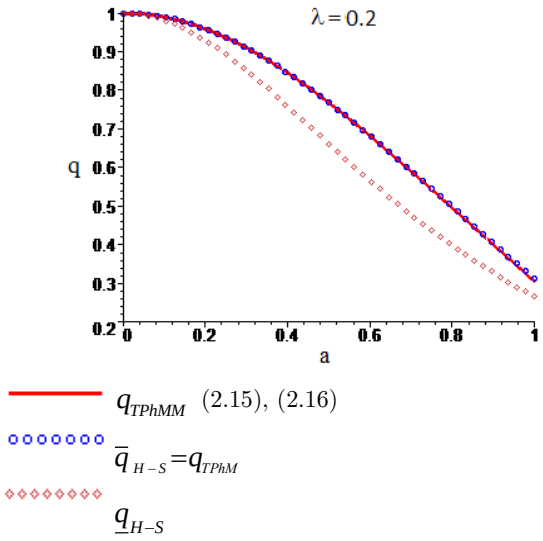

Fig. 4.3. Homogenized heat transfer coefficient for $\lambda = 0.2$.

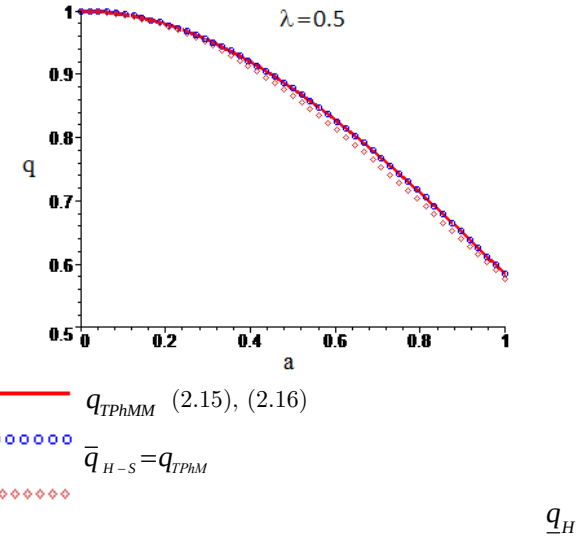

Fig. 4.4. Homogenized heat transfer coefficient for $\lambda = 0.5$.

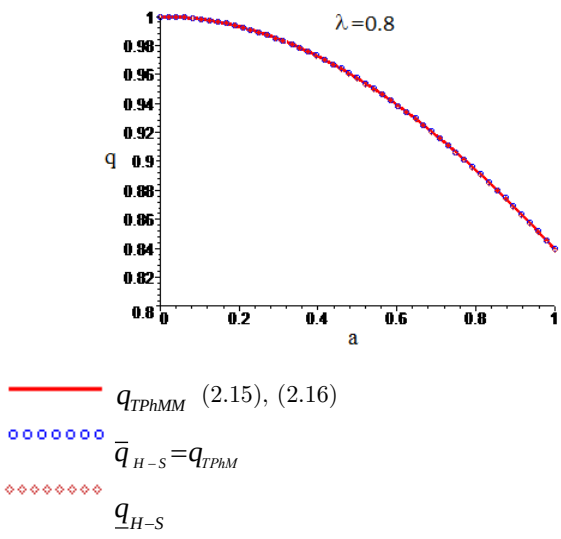

Fig. 4.5. Homogenized heat transfer coefficient for $\lambda = 0.8$.

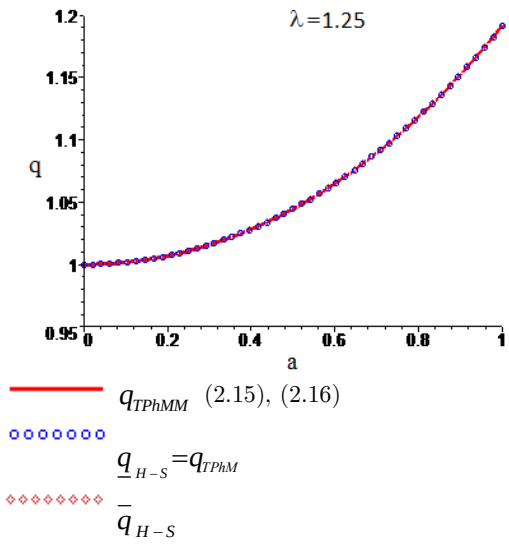

Fig. 4.6. Homogenized heat transfer coefficient for $\lambda = 1.25$.

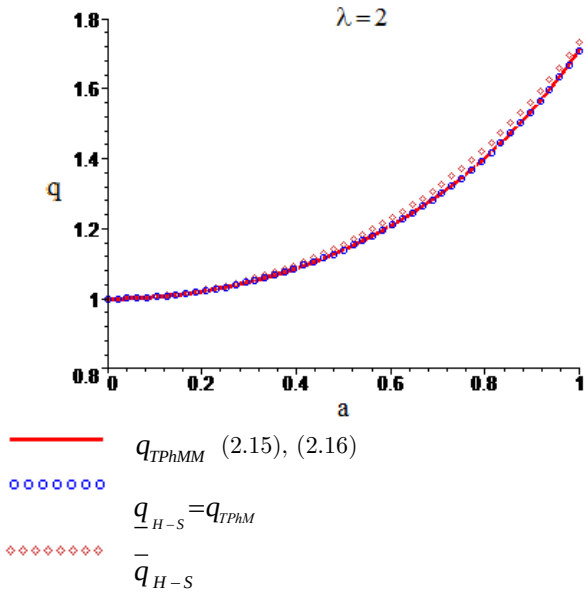

Fig. 4.7. Homogenized heat transfer coefficient for $\lambda = 2$.

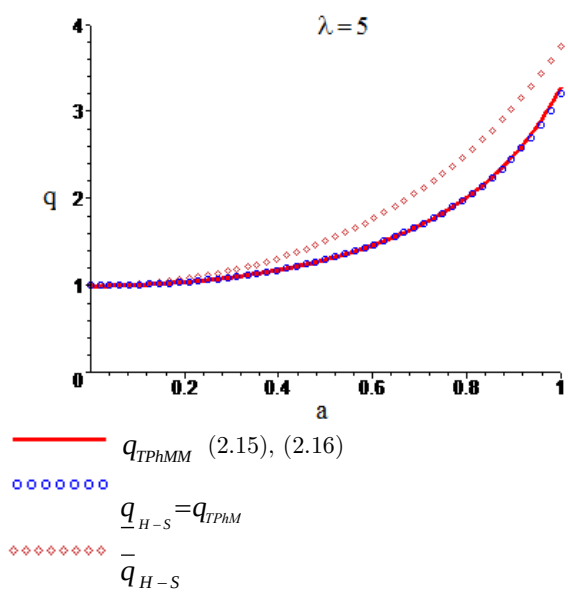

Fig. 4.8. Homogenized heat transfer coefficient for $\lambda = 5$.

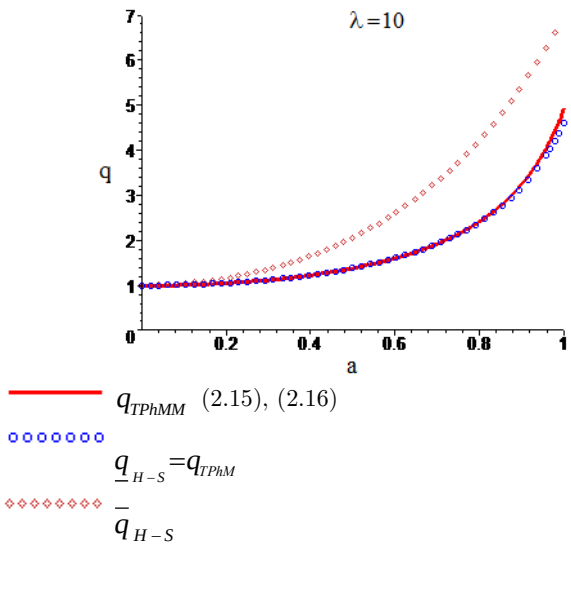

Fig. 4.9. Homogenized heat transfer coefficient for $\lambda = 10$.

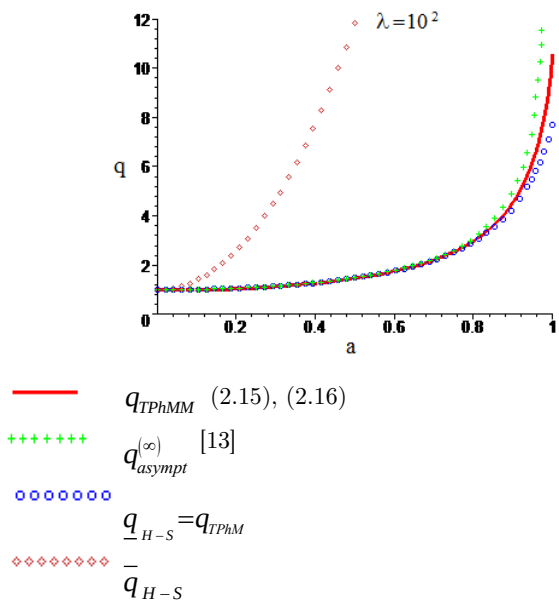

Fig. 4.10. Homogenized heat transfer coefficient for $\lambda = 10^2$.

2) Graphs related to the cases of geometrically large inclusions $a \to 1$, and either large $\lambda \to \infty$ or small $\lambda \to 0$ heat homogenized transfer coefficients and that computed by the TPhMM as well as those obtained in [9,13] are shown in Figures 4.11 - 4.14. The asymptotic solution obtained in [13] is as follows

$$q_{asympt}^{\infty} = \frac{\pi}{\sqrt{1-a^2}} - \pi + 1 \text{ for } \lambda \to \infty,\ a \to 1, \tag{4.3}$$

whereas that obtained in [9, 13] has the following form

$$q_{asympt}^{0} = \frac{\sqrt{1-a^2}}{\pi - \ \pi - 1\ \sqrt{1-a^2}} \text{ for } \lambda \to 0,\ a \to 1. \tag{4.4}$$

While constructing the dependencies shown in Figures 4.1 to 4.10, a solution to the transcendental Eqs. (2.15) and (2.16) has been found numerically, whereas dependencies in the vicinity of the limiting values of parameters $\lambda \to \infty, a \to 1$ and $\lambda \to 0, a \to 1$ (Figures 4.11 to 4.14) have been constructed with the help of asymptotic formulas (2.2) and (2.4), respectively.

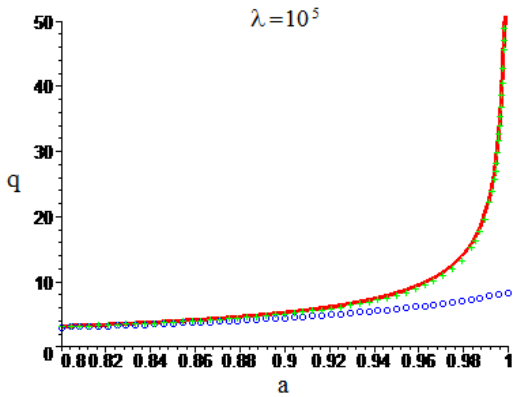

q_{TPhMM} (3.2)

$q_{asympt}^{(\infty)}$ [13]

q_{H-S}=q_{TPhM}

Fig. 4.11. Homogenized heat transfer coefficient for $\lambda = 10^5,\ a \to 1$.

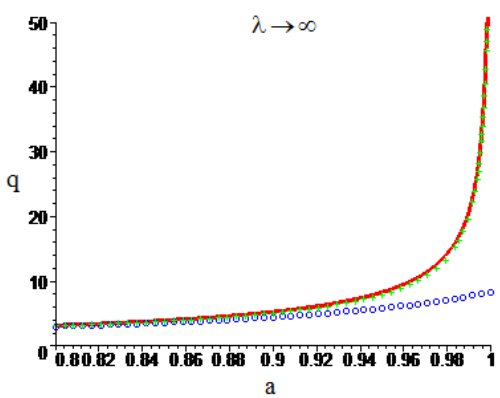

q_{TPhMM} (3.2)

$q_{asympt}^{(\infty)}$ [13]

q_{H-S}=q_{TPhM}

Fig. 4.12. Homogenized heat transfer coefficient for $\lambda \to \infty$, $a \to 1$.

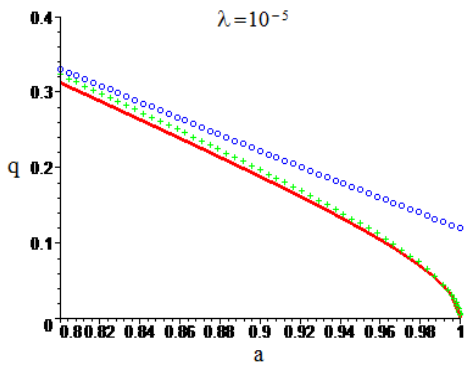

q_{TPhMM} (3.4)

$q^{(0)}_{asympt}$ [9,13]

$\overline{q}_{H-S}=q_{TPhM}$

Fig. 4.13. Homogenized heat transfer coefficient for $\lambda = 10^{-5}$, $a \to 1$.

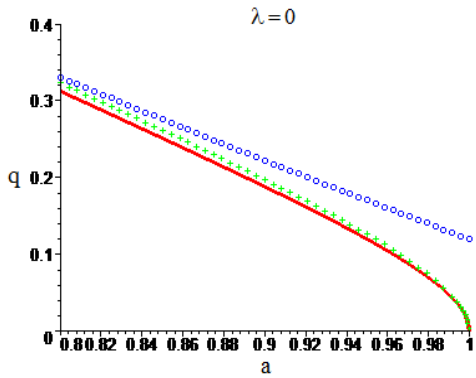

q_{TPhMM} (3.4)

$q^{(0)}_{asympt}$ [9,13]

$\overline{q}_{H-S}=q_{TPhM}$

Fig. 4.14. Homogenized heat transfer coefficient for $\lambda = 0$, $a \to 1$.

3) For small size of the inclusions $a << 1$ and various values of heat transfer λ the equivalent heat transfer parameter obtained through TPhMM in comparison to the Schwarz alternating method [1] are given in Figures 4.15 to 4.22.

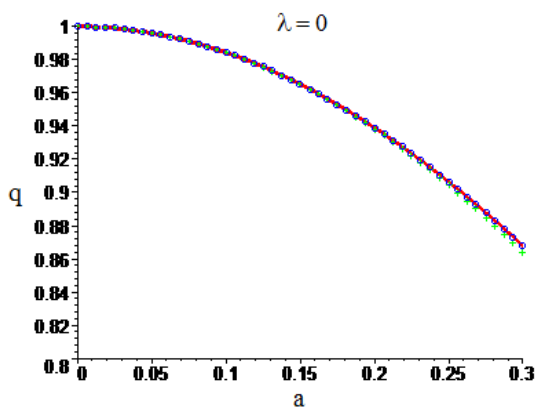

q_{TPhMM} (2.15), (2.16)

Schwarz method [1]

$\overline{q}_{H-S}=q_{TPhM}$

Fig. 4.15. Homogenized heat transfer coefficient for $\lambda = 0$, $a << 1$.

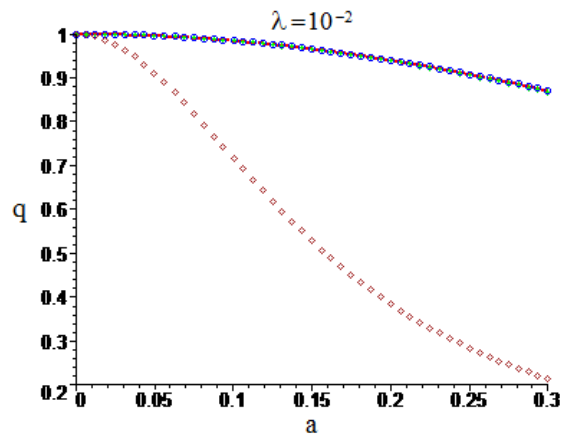

q_{TPhMM} (2.15), (2.16)

Schwarz method [1]

$\overline{q}_{H-S}=q_{TPhM}$

$\underline{q}_{H-S}$

Fig. 4.16. Homogenized heat transfer coefficient for $\lambda = 10^{-2}$, $a << 1$.

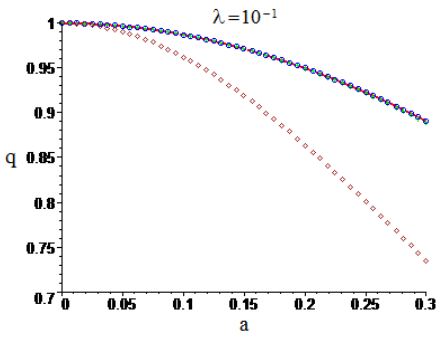

q_{TPhMM} (2.15), (2.16)

Schwarz method [1]

$\overline{q}_{H-S}=q_{TPhM}$

$\underline{q}_{H-S}$

Fig. 4.17. Homogenized heat transfer coefficient for $\lambda = 10^{-1}$, $a << 1$.

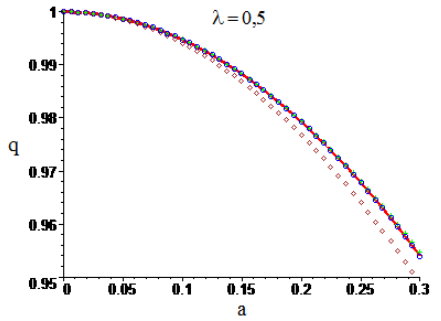

q_{TPhMM} (2.15), (2.16)

Schwarz method [1]

$\overline{q}_{H-S}=q_{TPhM}$

$\underline{q}_{H-S}$

Fig. 4.18. Homogenized heat transfer coefficient for $\lambda = 0.5$, $a << 1$.

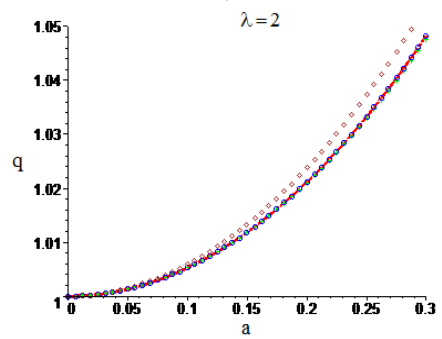

q_{TPhMM} (2.15), (2.16)

Schwarz method [1]

$\underline{q}_{H-S}=q_{TPhM}$

$\overline{q}_{H-S}$

Fig.4.19. Homogenized heat transfer coefficient for $\lambda = 2$, $a << 1$.

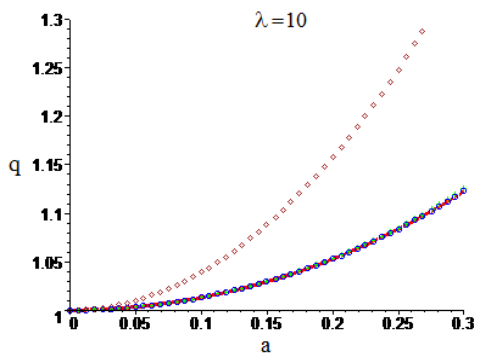

q_{TPhMM} (2.15), (2.16)

Schwarz method [1]

$\underline{q}_{H-S}=q_{TPhM}$

$\overline{q}_{H-S}$

Fig. 4.20. Homogenized heat transfer coefficient for $\lambda = 10$, $a << 1$.

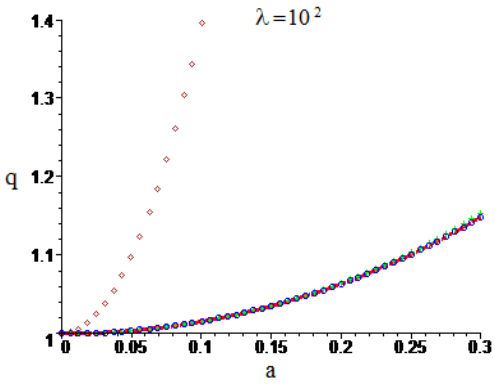

q_{TPhMM} (2.15), (2.16)

Schwarz method [1]

$\underline{q}_{H-S}=q_{TPhM}$

$\bar{q}_{H-S}$

Fig. 4.21. Homogenized heat transfer coefficient for $\lambda = 10^2$, $a << 1$.

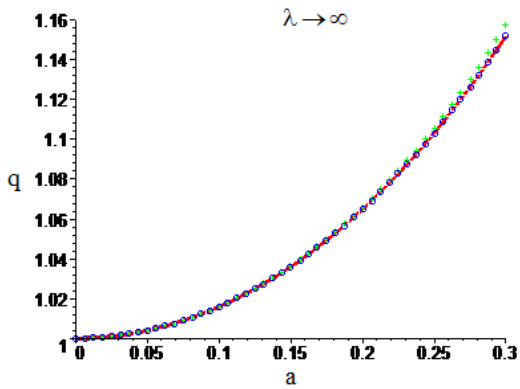

q_{TPhMM} (2.15), (2.16)

Schwarz method [1]

$\underline{q}_{H-S}=q_{TPhM}$

$\bar{q}_{H-S}$

Fig. 4.22. Homogenized heat transfer coefficient for $\lambda \to \infty$, $a << 1$.

4) Figures 4.23 to 4.26 give the dependencies of the homogenized heat transfer coefficient obtained through the TPhMM for various values of the inclusions size a. Namely, we have small inclusions: $a = 0.2$ (Fig. 4.15), inclusions of average size: $a = 0.4$; $a = 0.6$ (Figs. 4.16 and 4.17), large inclusions: $a = 0.8$ (Fig. 4.18).

Upper $\bar{q}_{H-S}$ and lower $\underline{q}_{H-S}$ Hashin-Shtrickman boundaries are marked, and the TPhM solution coinciding with $\underline{q}_{H-S}$ for $1 \le \lambda < \infty$ and with $\bar{q}_{H-S}$ for $0 \le \lambda \le 1$ is given.

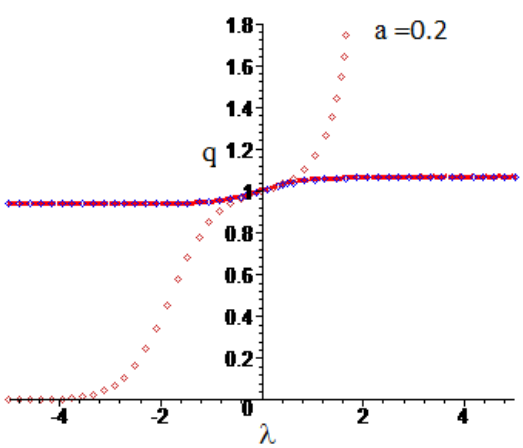

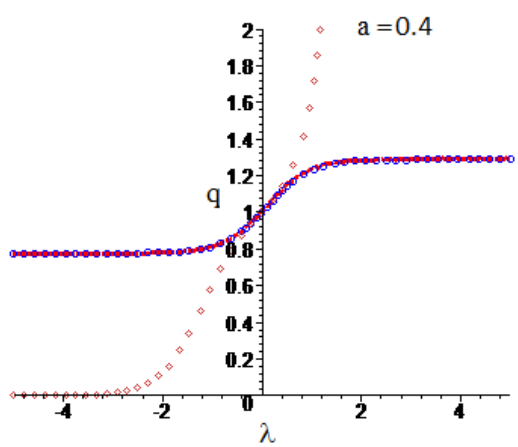

q_{TPhMM} (2.15), (2.16)

$q_{H-S}=q_{TPhM}$

q_{H-S}

Fig. 4.23. Homogenized heat transfer coefficient for $a = 0.2$.

q_{TPhMM} (2.15), (2.16)

$q_{H-S}=q_{TPhM}$

q_{H-S}

Fig. 4.24. Homogenized heat transfer coefficient for $a = 0.4$.

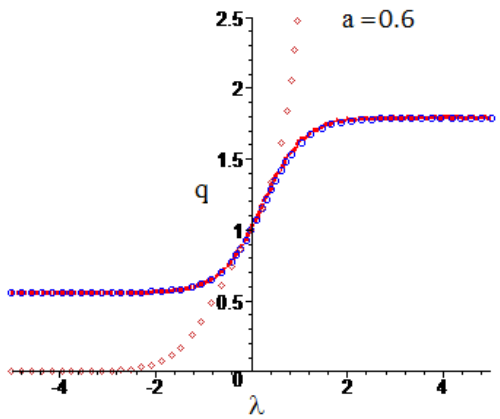

q_{TPhMM} (2.15), (2.16)

$q_{H-S}=q_{TPhM}$

q_{H-S}

Fig. 4.25. Homogenized heat transfer coefficient for $a = 0.6$.

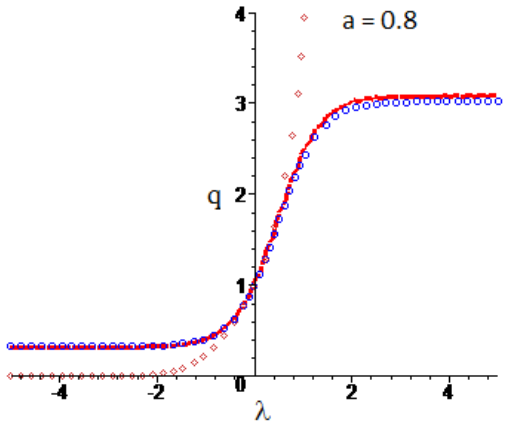

q_{TPhMM} (2.15), (2.16)

$q_{H-S}=q_{TPhM}$

q_{H-S}

Fig. 4.26. Homogenized heat transfer coefficient for $a = 0.8$.

5) Graphs shown in Figures 4.27 to 4.32 illustrate the behaviour of equivalent heat transfer coefficient versus conductivity λ of the inclusions of large size $a \to 1$. While constructing the graphs asymptotic formulas (2.15) and (3.7) have been used. In addition, the dependencies q^{∞}_{asympt} and q^{0}_{asympt}, constructed on the basis of (4.3) and (4.4), are added [9,13].

q_{TPhMM} (2.15) and (3.7)

$q^{(0)}_{asympt}$ [9,13]

$\bar{q}_{H-S}=q_{TPhM}$

Fig. 4.27. Homogenized heat transfer coefficient for $a = 0.99,\ 0 < \lambda \leq 1$.

q_{TPhMM} (2.15) and (3.7)

$q^{(\infty)}_{asympt}$ [13]

$\underline{q}_{H-S}=q_{TPhM}$

Fig. 4.28. Homogenized heat transfer coefficient for $a = 0.99,\ 1 \leq \lambda < \infty$.

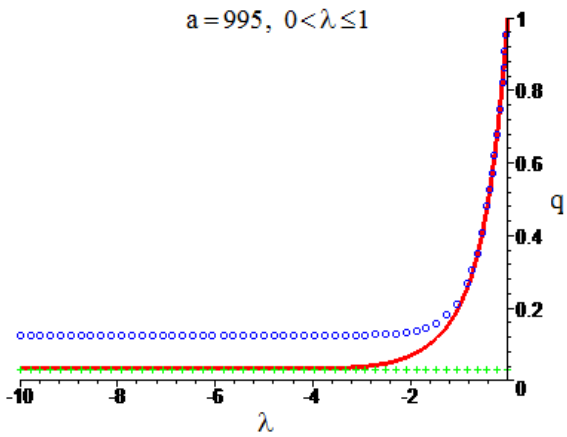

q_{TPhMM} (2.15) and (3.7)

$q^{(0)}_{asympt}$ [9,13]

$\overline{q}_{H-S} = q_{TPhM}$

Fig. 4.29. Homogenized heat transfer coefficient for $a = 0.995,\ 0 < \lambda \leq 1$.

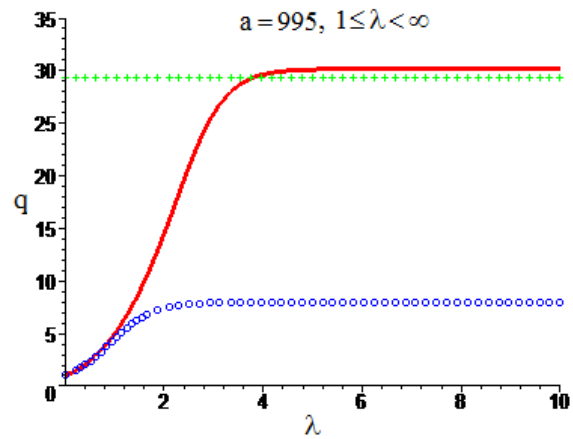

q_{TPhMM} (2.15) and (3.7)

$q^{(\infty)}_{asympt}$ [13]

$\underline{q}_{H-S} = q_{TPhM}$

Fig. 4.30. Homogenized heat transfer coefficient for $a = 0.995,\ 1 \leq \lambda < \infty$.

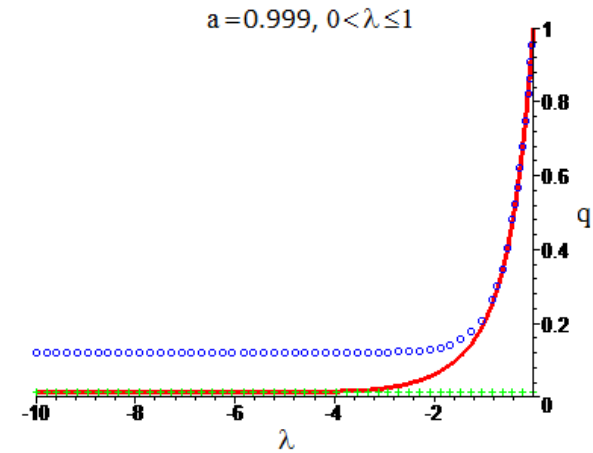

q_{TPhMM} (2.15) and (3.7)

$q^{(0)}_{asympt}$ [9,13]

$\overline{q}_{H-S} = q_{TPhM}$

Fig. 4.31. Homogenized heat transfer coefficient for $a = 0.999,\ 0 < \lambda \leq 1$.

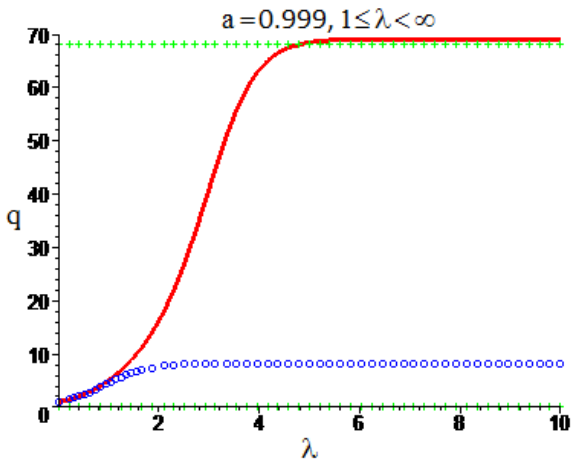

q_{TPhMM} (2.15) and (3.7)

$q^{(\infty)}_{asympt}$ [13]

$\underline{q}_{H-S} = q_{TPhM}$

Fig. 4.32. Homogenized heat transfer coefficient for $a = 0.999,\ 1 \leq \lambda < \infty$.

6) For the case of a composite structure with absolute heat transfer $\lambda \to \infty$ and of large size $a \to 1$ a comparison of the results regarding the effective computations of heat transfer coefficient found via the TPhMM with those reported by other authors are given in Tables 4.1 and 4.2.

Table 4.1. Numerical results of the estimation of heat transfer coefficient (absolutely conductive inclusions).

Inclusions concentration c / Inclusion size a	Series (3.9) [8]	Formula (3.12) [8]	Formula (3.13) [8]	Results [14]	Asymptotics [13]	TPhMM
0.1 / 0.3568	1.210	1.247	1.223	1.222	1.2214	1.2234
0.2 / 0.5046	1.470	1.544	1.506	1.500	1.4973	1.5065
0.3 / 0.6180	1.811	1.918	1.879	1.860	1.8546	1.8790
0.4 / 0.7136	2.306	2.417	2.395	2.351	2.3432	2.3955
0.5 / 0.7979	3.270	3.145	3.172	3.080	3.0700	3.1720
0.6 / 0.8740	7.106	4.386	4.517	4.342	4.3245	4.5175
0.7 / 0.9441	-	7.409	7.769	7.433	7.3857	7.7695
0.74 / 0.9707	–	10.91	11.46	11.01	10.9254	11.4624
0.76 / 0.9837	–	15.29	15.99	15.44	15.3284	15.9902
0.77 / 0.9901	–	20.18	21.04	20.43	20.2952	21.0488
0.78 / 0.9966	–	35.01	36.60	35.93	35.7525	36.6519

Table 4.2. Numerical and analytical results of the estimation of heat transfer coefficient (absolutely conductive inclusions).

Parameter $1/\sqrt{1-a^2}$ / Inclusion size a	Numerical computation [13]	Asymptotics [13]	TPhMM
10	29.4440	29.2743	30.1283

0.9949874370			
20	60.8976	60.6903	61.6814
0.9987492180			
30	92.3575	92.1062	93.1460
0.9994442899			
40	123.7734	123.5221	124.5868
0.9996874512			
50	155.1894	154.9380	156.0179
0.9997999801			
100	312.6460	312.0177	313.1276
0.9999499986			
1000	3142.5927	3142.5927	3140.9037
0.9999995001			

7) Table 4.3 gives computational results of the homogenized heat transfer coefficient obtained using the TPhMM and their comparison with the analytical solution given in reference [13] for the case of the inclusion size $0 << a < 1$ and large heat conductivity $0 << \lambda < \infty$.

Table 4.3. Computational results of the estimation of effective heat transfer coefficient (large size and large conductivity of inclusions).

Inclusion conductivity $\lambda = 10^2$			Inclusion conductivity $\lambda = 5 \cdot 10^2$		
Inclusion size a	Asymptotic solution [13]	TPhMM	Inclusion size a	Asymptotic solution [13]	TPhMM
0.9	4.9108	5.0044	0.9	5.0347	5.2456
0.91	5.2473	5.3449	0.91	5.3980	5.6282
0.92	5.6413	5.7411	0.92	5.8277	6.0792
0.93	6.1112	6.2097	0.93	6.3467	6.6213
0.94	6.6841	6.7753	0.94	6.9901	7.2893
0.95	7.4037	7.4765	0.95	7.8164	8.1407
0.96	8.3438	8.3770	0.96	8.9315	9.2776
0.97	9.6432	9.5934	0.97	10.5536	10.9067
0.98	11.5936	11.3680	0.98	13.2351	13.5334
0.99	14.8171	14.3260	0.99	19.0663	18.9367
0.991	15.2200	14.7431	0.991	20.1058	19.8518
0.992	15.6149	15.1940	0.992	21.3187	20.8999
0.993	15.9721	15.6836	0.993	22.7595	22.1169
0.994	16.2297	16.2179	0.994	24.5101	23.5539
0.995	16.2513	16.8041	0.995	26.7012	25.2868
Heat transfer of inclusions $\lambda = 10^3$			Heat transfer of inclusions $\lambda = 10^5$		
Inclusion	Asymptotic	TPhMM	Inclusion	Asymptotic	TPhMM

size a	solution [13]		size a	solution [13]	
0.9	5.0502	5.2776	0.9	5.0656	5.3099
0.91	5.4168	5.6661	0.91	5.4355	5.7043
0.92	5.8510	6.1249	0.92	5.8741	6.1709
0.93	6.3761	6.6774	0.93	6.4053	6.7342
0.94	7.0283	7.3605	0.94	7.0662	7.4325
0.95	7.8680	8.2343	0.95	7.9190	8.3297
0.96	9.0049	9.4080	0.96	9.0776	9.5418
0.97	10.6674	11.1050	0.97	10.7801	11.3109
0.98	13.4403	13.8868	0.98	13.6435	14.2620
0.99	19.5974	19.8425	0.99	20.1233	20.8685
0.991	20.7166	20.8903	0.991	21.3212	22.0828
0.992	22.0317	22.1070	0.992	22.7376	23.5164
0.993	23.6079	23.5437	0.993	24.4478	25.2448
0.994	25.5452	25.2763	0.994	26.5699	27.3860
0.995	28.0074	27.4232	0.995	29.3006	30.1366

8) In reference [1] for small inclusion size $a << 1$, the formula for equivalent heat transfer coefficient obtained using the Schwarz method of successive approximations is reported. Table 4.4 gives the computational results of homogenized heat transfer coefficient using ThPM [16] as well as the Schwarz method [1] and the TPhMM for the case of various heat transfer λ and small values of the inclusion size a.

Table 4.4. Computational results of the estimation of effective heat transfer coefficient (small size of inclusions).

Inclusion conductivity $\lambda = 0$				Inclusion conductivity $\lambda = 10^{-2}$			
Inclusion size a	TPhM [16]	Schwarz method [1]	TPhMM	Inclusion size a	TPhM [16]	Schwarz method [1]	TPhMM
0.05	0.9961	0.9961	0.9961	0.05	0.9962	0.9962	0.9962
0.1	0.9844	0.9844	0.9844	0.1	0.9847	0.9847	0.9847
0.15	0.9653	0.9650	0.9653	0.15	0.9659	0.9657	0.9659
0.2	0.9391	0.9382	0.9391	0.2	0.9403	0.9394	0.9402
0.25	0.9064	0.9044	0.9064	0.25	0.9082	0.9063	0.9082
0.3	0.8680	0.8639	0.8679	0.3	0.8704	0.8666	0.8704
Inclusion conductivity $\lambda = 10^{-1}$				Inclusion conductivity $\lambda = 0.5$			
Inclusion size a	TPhM [16]	Schwarz method [1]	TPhMM	Inclusion size a	TPhM [16]	Schwarz method [1]	TPhMM
0.05	0.9968	0.9968	0.9968	0.05	0.9987	0.9987	0.9987
0.1	0.9872	0.9872	0.9872	0.1	0.9948	0.9948	0.9948
0.15	0.9715	0.9714	0.9715	0.15	0.9883	0.9883	0.9883
0.2	0.9499	0.9494	0.9499	0.2	0.9793	0.9794	0.9793

0.25	0.9228	0.9218	0.9228	0.25	0.9678	0.9681	0.9678
0.3	0.8907	0.8887	0.8906	0.3	0.9540	0.9546	0.9540
Inclusion conductivity $\lambda = 2$				Inclusion conductivity $\lambda = 10$			
Inclusion size a	TPhM [16]	Schwarz method [1]	TPhMM	Inclusion size a	TPhM [16]	Schwarz method [1]	TPhMM
0.05	1.0013	1.0013	1.0013	0.05	1.0032	1.0032	1.0032
0.1	1.0052	1.0052	1.0052	0.1	1.0129	1.0130	1.0129
0.15	1.0119	1.0118	1.0119	0.15	1.0293	1.0295	1.0293
0.2	1.0212	1.0210	1.0212	0.2	1.0528	1.0532	1.0528
0.25	1.0333	1.0329	1.0333	0.25	1.0839	1.0849	1.0837
0.3	1.0483	1.0475	1.0483	0.3	1.1228	1.1253	1.1228
Inclusion conductivity $\lambda = 10^2$				Inclusion conductivity $\lambda \to \infty$			
Inclusion size a	TPhM [16]	Schwarz method [1]	TPhMM	Inclusion size a	TPhM [16]	Schwarz method [1]	TPhMM
0.05	1.0039	1.0038	1.0039	0.05	1.0039	1.0039	1.0039
0.1	1.0155	1.0153	1.0156	0.1	1.0158	1.0159	1.0158
0.15	1.0353	1.0343	1.0355	0.15	1.0360	1.0363	1.0360
0.2	1.0635	1.0606	1.0645	0.2	1.0649	1.0659	1.0649
0.25	1.1011	1.0937	1.1034	0.25	1.1032	1.1057	1.1033
0.3	1.1489	1.1334	1.1539	0.3	1.1521	1.1575	1.1522

Table 4.5 gives the mean absolute discrepancy of the computation of effective heat transfer coefficient λ using the TPhMM versus known results obtained by other authors.

Table 4.5. Mean value of the absolute discrepancy of the estimation of heat transfer coefficient using the TPhMM and results obtained by other authors in %

1. Inclusions: Mean size : $0.3568 \le a \le 0.8740$; Absolute conductivity: $\lambda \to \infty$				
Formula (3.9) [8]	Formula (3.12) [8]	Formula (3.13) [8]	Results [14]	Asymptotics [13]
3.2790	2.3457	0.0119	2.4839	2.8573
2. Inclusions: Large size : $0.9441 \le a \le 0.9966$; Absolute conductivity: $\lambda \to \infty$				
Formula (3.12) [8]	Formula (3.13) [8]	Results [14]	Asymptotics [13]	
4.6594	0.0515	3.1776	3.8654	
3. Inclusions: Large size : $0.99498744 \le a \le 99999950$; Absolute conductivity: $\lambda \to \infty$				

Numerical computation [13]	Asymptotics [13]
0.5899	0.7884
4. Inclusions:	Large size : $0.9 \leq a \leq 995$ Large conductivity: $10^2 \leq \lambda \leq 10^5$
Asymptotics [13]	
3.1354	
5. Inclusions:	Small size : $0 \leq a \leq 0{,}3$ Non-conductivity: $\lambda = 0$
TPhM [16]	Schwarz method [1]
0.0016	0.1159
6. Inclusions:	Small size : $0 \leq a \leq 0.3$ Small conductivity: $10^{-2} \leq \lambda \leq 10^{-1}$
TPhM [16]	Schwarz method [1]
0.0016	0.0814
7. Inclusions:	Small size : $0 \leq a \leq 0.3$ Matrix magnitude conductivity: $0.5 \leq \lambda \leq 2$
TPhM [16]	Schwarz method [1]
0.0000	0.0178
8. Inclusions:	Small size : $0 \leq a \leq 0{,}3$ Large conductivity: $10 \leq \lambda \leq 100$
TPhM [16]	Schwarz method [1]
0.0561	0.2585
9. Inclusions:	Small size : $0 \leq a \leq 0{,}3$ Absolute conductivity: $\lambda \to \infty$
TPhM [16]	Schwarz method [1]
0.0030	0.1346

5 CONCLUSIONS

One may conclude from the data reported in Table 4.1 and from the paper text body that our results constructed through the proposed improved TPhM allow us to improve the results obtained via the classical TPhM approach regarding the estimation of effective heat transfer parameter of the

composite structure with periodically located cylindrical inclusions of circular cross-sections on the square net.

Finally, let us emphasise that the TPhMM is practically validated and gives reliable results in the whole area of both composite parameters variation, i.e. with respect to:

(i) geometric parameter regarding the size of inclusions $a:\ 0 < a < 1$;

(ii) physical parameter regarding the inclusion conductivity $\lambda:\ 0 < \lambda < \infty$, including the limiting cases: $a \to 0$, $a \to 1$ and $\lambda \to 0$, $\lambda \to \infty$.

References

1. I.V. Andrianov, G.A. Starushenko, Asymptotic methods in the theory of perforated membranes of nonhomogeneous structure, Eng. Trans. 43 (1995) 5-18.
2. I.V. Andrianov, G.A. Starushenko, V.V. Danishevs'kyy, S. Tokarzewski, Homogenization procedure and Padé approximations in the theory of composite materials with parallelepiped inclusions, Int. J. Heat Mass Transfer 41(1) (1998) 175-181.
3. I.V. Andrianov, G.A. Starushenko, V.V. Danishevs'kyy, S. Tokarzewski, Homogenization procedure and Padé approximants for effective heat conductivity of composite materials with cylindrical inclusions having square cross-section, Proc. R. Soc. A 455 (1999) 3401-3413.
4. R.M. Christensen, Mechanics of Composite Materials, Dover Publications, Mineola, New York, 2005.
5. R.M. Christensen, K.H. Lo, Solutions for effective shear properties in three phase sphere and cylinder models, J. Mech. Phys. Solids 27 (1979) 315-330.
6. Z. Hashin, S. Shtrikman, A variational approach to the theory of the effective magnetic permeability of multiphase materials, J. Math. Phys. 33 (1962) 3125-3131.
7. Z. Hashin, S. Shtrikman, A variational approach to the theory of the elastic behaviour of multiphase materials, J. Mech. Phys. Solids 11 (1963) 127-140.
8. A.L. Kalamkarov, I.V. Andrianov, V.V. Danishevs'kyy, Asymptotic homogenization of composite materials and structures, Appl. Mech. Rev. 62(3) (2009) 030802-1 – 030802-20.
9. J.B. Keller, A theorem on the conductivity of a composite medium, J. Math. Phys. 5 (1964) 548-549.
10. E.H. Kerner, The electrical conductivity of composite media, Proc. Physics Soc. B 69(8), (1956) 802-807.
11. E.H. Kerner, The elastic and thermoelastic properties of composite media, Proc. Physics Soc. B 69(8) (1956) 808-813.
12. J.-L. Lions, On some homogenisation problem, ZAMM 62(5) (1982) 251-262.
13. R.C. McPhedran, L. Poladian, G.W. Milton, Asymptotic studies of closely spaced, highly conducting cylinders, Proc. R. Soc. A 415 (1988) 185-196.
14. W.T. Perrins, D.R. McKenzie, R.C. McPhedran, Transport properties of regular arrays of cylinders, Proc. R. Soc. A 369 (1979) 207-225.
15. G.A. Starushenko, B.E. Rogoza, Review and analysis of three-phase model in mechanics of composites, Part I, Systems Technol., Dnepropetrovsk 5(52) (2007) 3-10 (in Russian).
16. G.A. Starushenko, B.E. Rogoza, Review and analysis of three-phase model in mechanics of composites, Part II, Systems Technol., Dnepropetrovsk 1(54) (2008) 3-12 (in Russian).
17. C. Van der Poel, On the rheology of concentrated dispersions, Rheol. Acta 1(2-3) (1958) 198-205.
18. V.V. Zhikov, Estimates for the averaged matrix and the averaged tensor, *Russ. Math. Surv.* 46(3) (1991) 65-136